

Modified Microstrip Feed Hybrid Rectangular Dielectric Resonator Antenna for Wireless Tri-Band Applications

Chaitanya B*, Manjunathachari K

Department of Electrical, Electronics & Communication Engineering, GITAM School of Technology, Hyderabad Campus, Telangana, India, bchaitanya55@yahoo.com, mkamsali@gitam.edu

Abstract: This article reports the Modified Microstrip Feed Hybrid Rectangular Dielectric Resonator Antenna (RDRA). The proposed structure has a ground plane with a plus-shaped slot on an FR4 substrate with a height of 1.6 mm and dimensions of 38 mm x 35 mm. The proposed Dielectric resonator antenna is made of a material with 10 as its dielectric constant, and the dimensions of the DR are 19 x 20 x 18 mm³. The DR is connected to a modified microstrip feed with an octagonal ring through the plus-shaped slot in the ground. The proposed structure operates in frequencies from 2.60 GHz - 2.74 GHz, 3.12 GHz - 3.37 GHz, and 4.25 GHz - 4.37 GHz. The resonant frequency of the final proposed RDRA is 2.68 GHz, 3.26 GHz, and 4.31 GHz, which covers WLAN, WIMAX and Wireless Avionics Intra-Communications (WAIC) applications, respectively. The entire structure was simulated using the CST microwave studio. The simulated results agree with the measured results and both are presented. The compact size, stable radiation pattern and reasonable gain make this antenna suitable for the proposed applications.

Keywords: Rectangular dielectric antenna, WLAN, WIMAX, WAIC, Hybrid DRA, multi-band, compact size.

1. INTRODUCTION

Researchers often use the Dielectric Resonator Antenna (DRA) [1] because of its excellent advantages such as wider bandwidth with reasonable efficiency, low cost with very low fabrication complexity, and high gain [2], [3]. DRA has overcome all the disadvantages of the conventional and other new printed antenna techniques because it has unique characteristics such as flexibility, very low conductor losses, and excellent radiation performance [4], [5]. The DRA may be of any shape. Circular, square, and rectangular shapes are widely used due to their fabrication simplicity, with the rectangular DRA being the most commonly used due to its two-degree freedom. The Rectangular DRA characteristics depend on the aspect ratio, and the DRA can also be excited by different feeding techniques. In the current advancement of wireless technology, antennas with multiband characteristics play an important role. A large number of narrowband applications such as Wireless Local Area Network (WLAN), Worldwide Interoperability for Microwave Access (WIMAX), Long Term Evolution (LTE) and other standards are being deployed. In the last decade, the most needed part of communication devices is the single antenna that works with multiple wireless communication standards. By integrating such multi-band antennas, the communication devices become smaller.

The DRA has been widely used to achieve multi-band characteristics since the last decade due to its desired band

coverage and undesired band rejection capability. Parasitic elements [6], multi-band excitation with unique feeding strips [7], [8], [24], [25], or hybrid [9]-[11] techniques are commonly used to achieve the multi-band characteristics along with DRA. Fractal DRA is proposed for wideband application [11], [12] and multi-band application [13]. Co-Planar Waveguide (CPW) feeding is widely used to achieve multi-band characteristics due to its very low dispersion and radiation losses. But all the above methods are complex in terms of fabrication and size. Multi-band can also be achieved by combining two or more DRAs. In this case, two elements must operate in the same mode at different frequencies. The combined effect of the DRAs allows multi-band operation with good impedance matching, but the major drawback is the need of a large sized DR, so it cannot be used for modern wireless communication devices. Ring structures are often used as patches because of their radiation effects. Closed ring resonators and open ring resonators are used as patches in hybrid DRA to achieve good impedance matching and a multi-band effect. In multimode techniques [14], [15], independent frequency control is not possible because only the DRA radiates. In [16] a multiple DRA is proposed for wide multi-band operation, in [17] a cylindrical DRA with filters for wireless applications.

The above-mentioned shortcomings can be overcome by Hybrid DRA (HDRA), in which a radiator or microstrip patch is used together with DRA. Independent frequency control

and higher band achievement are two major advantages of hybrid DRA. In this paper, Hybrid Rectangular DRA (HRDRA) with triple-band operation is proposed for WLAN, WIMAX, and Wireless Avionics Intra-Communications (WAIC) applications. The antenna is coupled by two orthogonal slots and excited with two microstrip rectangular ring slots.

2. RDRA GEOMETRY

The proposed RDRA is shown in Fig. 1. The RDRA consists of Arlon with 10 as its dielectric constant and the loss tangent 0.0023. The designed RDRA has a width of x , a length of b , and a height of h_1 . The RDRA is placed over the plus-shaped slot that is imprinted into the ground plane. The substrates hold the ground plane and the substrate is made of FR4 with 4.4 as its dielectric constant and 0.002 loss tangent. The substrate has dimensions of w for width, l for length, and h for height. On another adjacent of the substrate, the microstrip octagonal feed structure is printed to excite the whole structure. The microstrip has a feed width of fw and a feed length of fl . The octagonal ring has two rings. The outer and inner rings have outer radii of 10 mm and 8.5 mm, respectively. The ring thickness of both rings is 1 mm. The gap between the two rings is 0.5 mm wide. The plus-shaped slot with a length of l_1 and a thickness of 1.1 mm is created in the ground. The dimension of the RDRA can be calculated by the following equation [1], [2].

$$k_0 = 2\pi f_0 / C \quad (1)$$

$$k_x^2 + k_y^2 + k_z^2 = \epsilon k_0^2 \quad (2)$$

In the above equation, f_0 is the resonant frequency, C is the speed of light. The wavenumber in the x , y , and z -directions is represented by K_x , K_y , and K_z , respectively. The RDRA parameters are optimized using CST Microwave Studio software. The final parameters are shown in Fig. 2, and their values are listed in Table 1. The radiation patterns are not symmetrical because the RDRA is not placed in the center of the ground plane. The lowest resonant frequency of the designed RDRA is the fundamental mode TE_{116} , which was designed according to the DWM method [18].

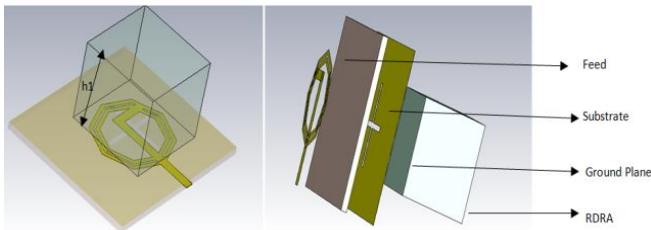


Fig. 1. RDRA geometry.

Table 1. Parameter values (in mm).

w	l	x	b	fl	fw
38	35	19	20	23	2.2
l1	v	t	s	11	h1
1.1	6.7	1	10	16	18

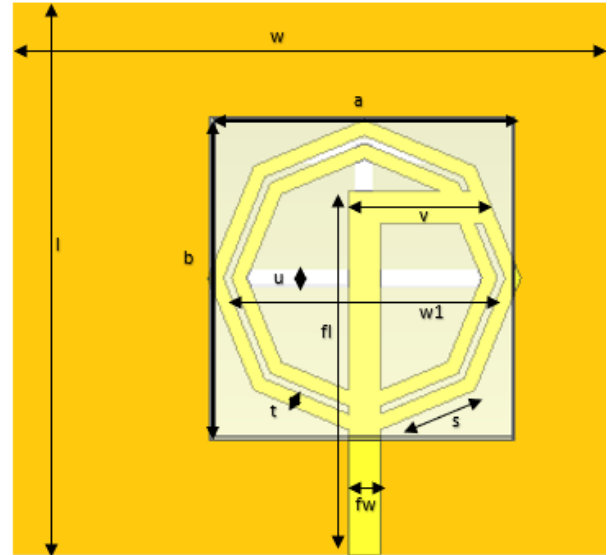


Fig. 2. RDRA with its parameters.

Feed geometry design process

The shape of the feed is crucial because it facilitates the coupling of all electromagnetic energy into the dielectric resonator antenna. The altered feed configuration starts with a basic microstrip that does not effectively link the energy to the DRA. Therefore, an octagonal ring is introduced to provide impedance matching. The combination of the microstrip line and the octagonal ring, referred to as Feed 1, operates across three distinct frequency bands. However, it exhibits inadequate impedance matching for the higher-order modes. To address this, a small stub is used to connect the microstrip line and the octagonal ring, creating Feed 2. However, this feed structure reduces the impedance for the lower mode. As a solution, another ring with a stub connection (Feed 3) is implemented in the final design, resulting in a flawless impedance match.

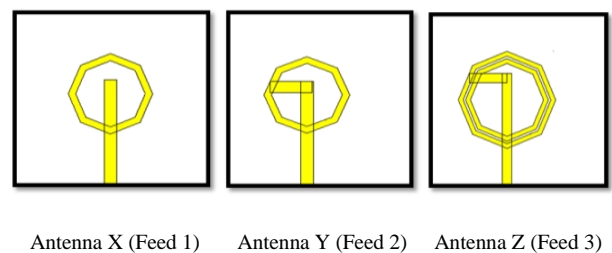


Fig. 3. Feed evolution.

Fig. 3 illustrates the progression of the feed design. Fig. 4 shows a comparison of S_{11} values for different feed structures. The results show that with Feed 1, the proposed RDRA operates in the frequency ranges of 2.63 GHz to 2.83 GHz, 3.3 GHz to 3.50 GHz, and 4.73 GHz to 4.83 GHz. However, impedance matching is notably low in the two upper bands. When using Feed 2, the designed RDRA operates between 2.66 GHz and 2.76 GHz, 3.30 GHz and 3.54 GHz, and 4.61 GHz and 4.71 GHz. Unfortunately, the impedance of the lower resonance is not adequately matched. Feed 3, on the other hand, shows excellent impedance matching across all frequency bands, operating from

2.60 GHz to 2.74 GHz, 3.12 GHz to 3.37 GHz, and 4.25 GHz to 4.37 GHz. The resonant frequencies for the final proposed RDRA are 2.68 GHz, 3.26 GHz, and 4.31 GHz, covering applications in WLAN, WiMAX, and WAIC.

Fig. 5 shows the S11 values for the feed structure without the DRA. They clearly show that the rectangular dielectric used contributes significantly to the achievement of triband operation. The resonating modes $TE_{X\delta 10}$, $TE_{X\delta 11}$, and TE_{X111} occur at 2.68 GHz, 3.26 GHz, and 4.31 GHz, respectively. Moreover, the far-field distribution of the short magnetic dipole matches the $TE_{X\delta 11}$ characteristics, with all radiation patterns exhibiting omnidirectional traits.

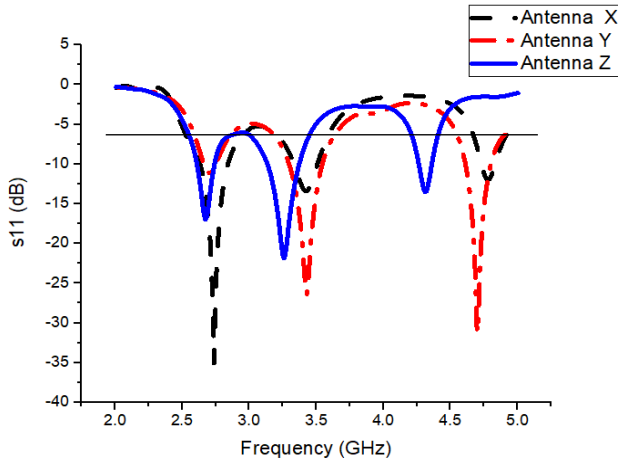


Fig. 4. Return loss comparison plot.

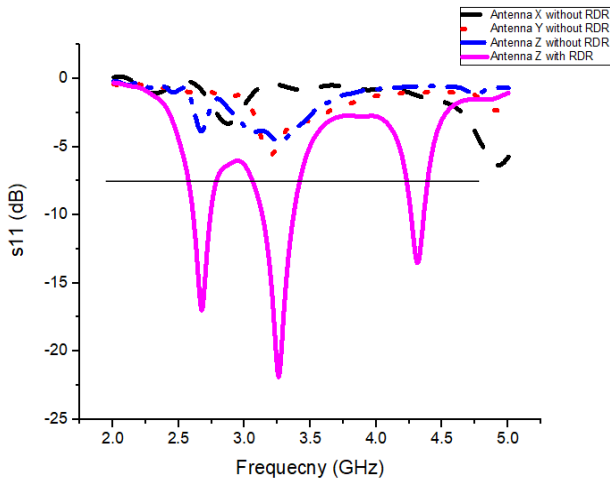


Fig. 5. Return loss comparison plot with and without DR.

3. PARAMETRIC ANALYSIS

The parametric study is used to find the optimum dimension of the designed antenna and to study the performance features of the designed RDRA.

The feed width is the critical parameter that has a greater impact on impedance matching and resonant frequency. Therefore, its optimized values are determined using parametric analysis. The feed width is increased from 1.8 to 2.6 mm in steps of 0.4 mm. The return loss performance of RDRA for different feed widths is shown in Fig. 6. Fig. 6

shows that the 2.2 mm has very good impedance matching and therefore is chosen for the final fabrication. The slot length l_1 also has a great impact on the impedance matching. The l_1 is increased in steps of 0.2 mm from 0.9 mm to 1.3 mm. From Fig. 7, which shows the comparison of s11 for different slot lengths, it can be seen that when the l_1 is increased, the impedance matching at $l_1 = 1.1$ mm is appropriate and therefore chosen for the fabrication.

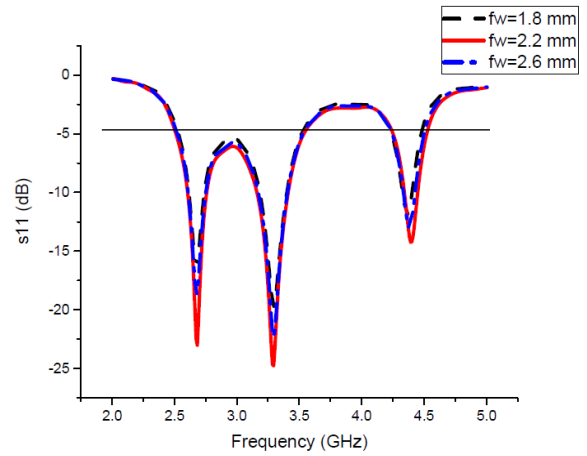


Fig. 6. Return loss comparison plot for different feed widths fw.

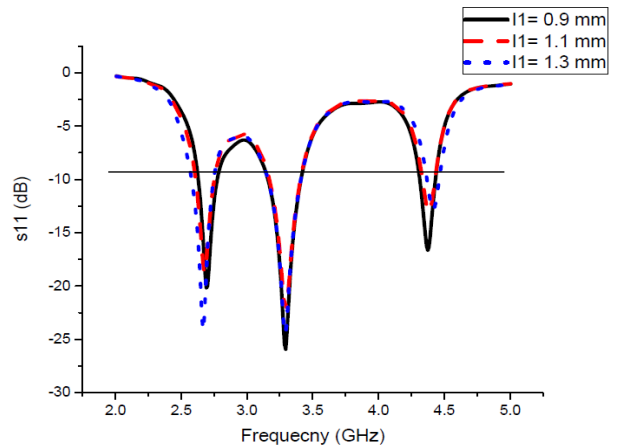


Fig. 7. Return loss comparison plot for different slot lengths l1.

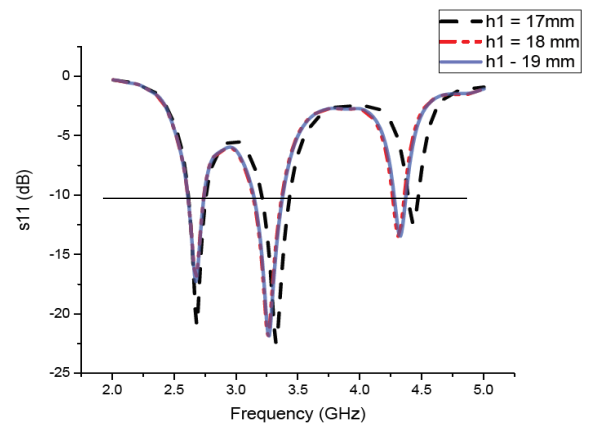


Fig. 8. Return loss comparison plot for different DRA heights h1.

The DRA [19]-[21] dimension will have a more noteworthy influence on the routine of the proposed RDRA, so its height and width will be considered for the analysis. The height of the DR is increased from 17 mm to 19 mm in steps of 1 mm, the height $h_1 = 18$ mm has excellent impedance and resonance tuning, and therefore is chosen for final fabrication. The width of the DR is also increased in steps of 2 mm from 17 mm to 21 mm. From Fig. 9 it can be seen that a width of 19 mm covers the required resonance with good impedance bandwidth and matching. Therefore, a dielectric resonator with a height of 18 mm and a width of 19 mm is chosen for the final fabrication.

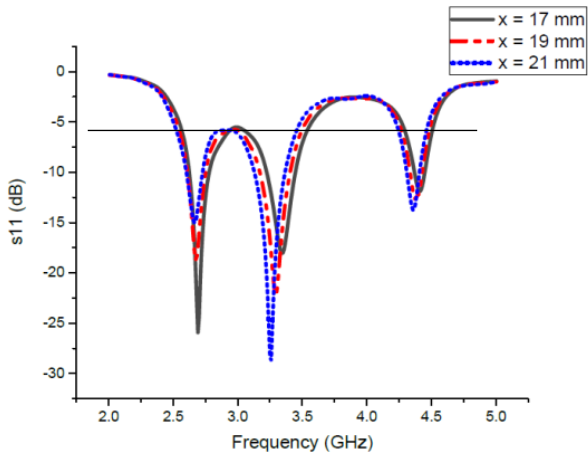


Fig. 9. Return loss comparison plot for different DRA widths.

4. RESULTS AND DISCUSSION

Fig. 10 shows the surface current of the designed RDRA. It can be observed that the surface current rotates from the left to the right side at all resonant frequencies. The maximum surface current is concentrated on the feed geometry and around the ring structure coupling with the DRA.

Fig. 11 shows that the surface current in the ground plane at 3.26 GHz is plotted from phase 0 degrees and 90 degrees. It can be observed that the E-field also shifts from left to right when the phase is shifted from zero degrees to ninety degrees. From rotation of the electric field, we can conclude that the proposed structure operates in TE_{118} mode.

The proposed RDRA is fabricated by stacking the dielectric on top of each other, since the required height is not available. The s_{11} is measured using Agilent E5071C VNA.

The radiation pattern at different resonating frequencies is shown in Fig. 12. The E-plane has a dipole antenna radiation pattern and the H-plane has an omnidirectional pattern. Both the E- and H-planes have a stable radiation pattern. The measured results are closer to the simulated results. The simulated s_{11} is compared and presented with the measured s_{11} in Fig. 13. The slight deviation between the results is due to manufacturing and SMA connection errors.

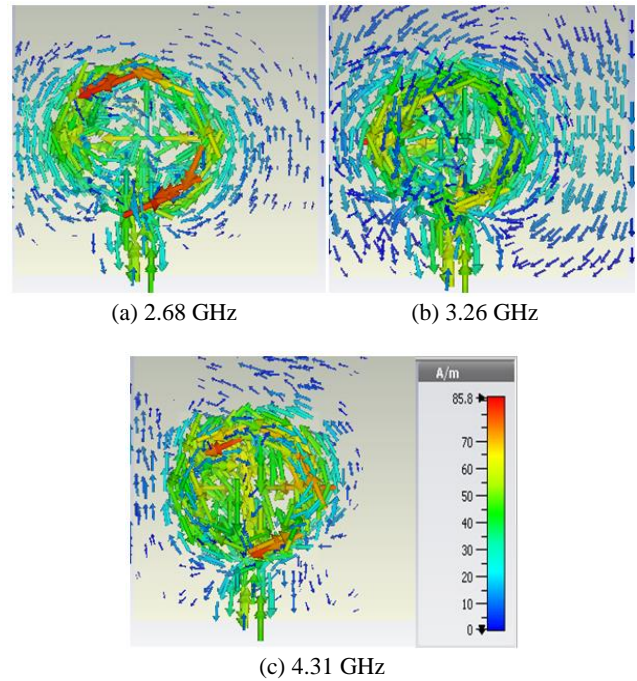


Fig. 10. Surface current distribution at different resonant frequencies.

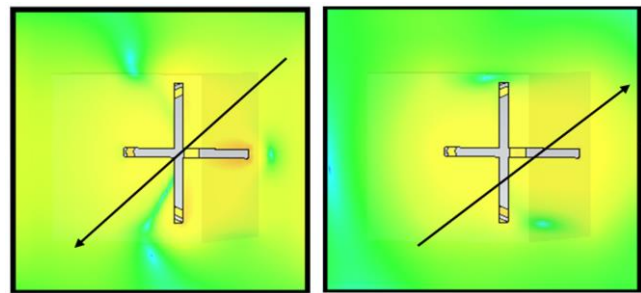


Fig. 11. Surface current distribution at 3.26 GHz, phase 0 & 90 degrees.

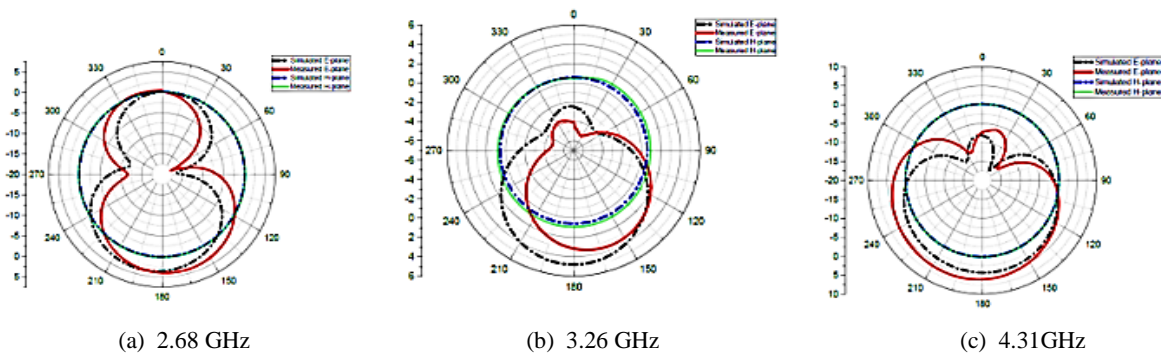


Fig. 12. E-plane and H-plane radiation pattern.

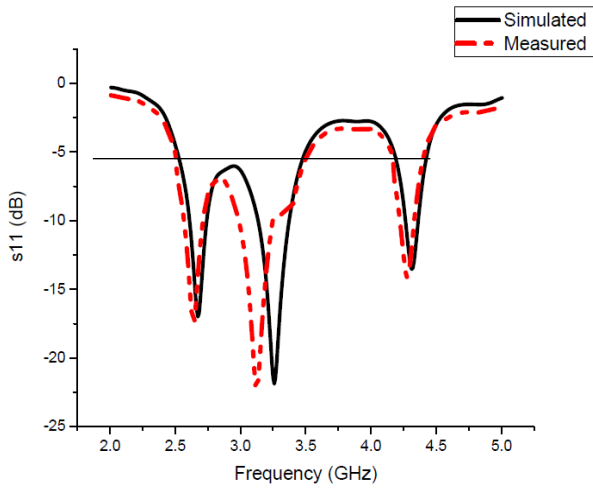


Fig. 13. Simulated vs measured s11 characteristics.

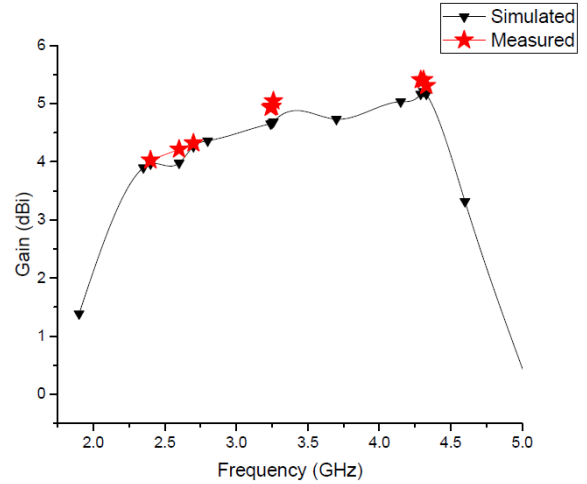


Fig. 14. Simulated vs measured gain.

Fig. 14 shows the simulated vs measured gain. The maximum measured gain is 5.125 dBi. Table 2 compares the simulated and measured results. In Table 3, the previous reported RDRA is compared with the proposed RDRA, which clearly shows that the proposed RDRA outperforms the results published in the literature. Fig. 15 shows the fabricated antenna. The antenna was fabricated using the photolithography method.

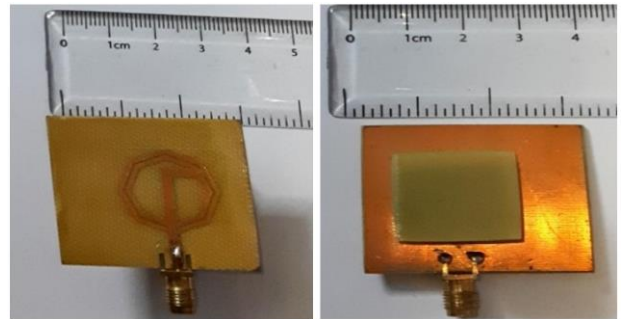


Fig. 15. Fabricated antenna.

Table 2. Measured vs. simulated results.

Band	Resonant frequency (GHz)		Operating frequency range (GHz)	
	Simulated	Measured	Simulated	Measured
Band 1	2.68	2.64	2.61 - 2.73	2.57 - 2.71
Band 2	3.26	3.12	3.142 - 3.36	2.98 - 3.20
Band 3	4.31	4.27	4.26 - 4.35	4.23 - 4.33

Table 3. Proposed antenna vs reported in literature.

Reference	DRA Geometry	Feeding Mechanism	ϵ_r (DRA)	Frequency Range	Total Size	Gain	Fabrication
19	Stacked rectangular DRA	Aperture	15, 2.2	3.94 - 6.06	$46 \times 46 \times 6.413$	10.5	Complex
20	E-shaped DRA	Microstrip	10.2	6.0 - 10.2	$50 \times 50 \times 15.762$	8.1	Complex
21	Half cylindrical DRA	Probe	9.8	5.1 - 8.3	$50 \times 50 \times 18$	5.94	Complex
22	Hybrid Monopole DRA	Probe	10	4.6 - 9.7	$r=4.2 \text{ mm} \ \& \ h=10 \text{ m}$	4	Complex
23	CDRA	Microstrip	9.8, 4.4	2.50 - 2.76, 3.38 - 3.54, 4.90 - 5.30, 5.50 - 5.61, 5.78 - 5.98	$40 \times 40 \times 14.6$	5.8	Complex
This work	Hybrid Rectangular DRA	Microstrip	10, 4.4	2.60 - 2.74, 3.12 - 3.37, 4.25 - 4.37	$32 \times 35 \times 19.6$	5.5	Easy

5. CONCLUSION

In this paper, a hybrid Rectangular DRA for tri-band operation is presented. The presented structure consists of a modified microstrip octagonal feed structure RDRA coupled with a plus-shaped slotted ground plane. The proposed structure operates from 2.60 GHz - 2.74 GHz, 3.12 GHz-3.37 GHz, and 4.25 GHz-4.37 GHz. The resonant frequency of the final proposed RDRA is 2.68 GHz, 3.26 GHz, and 4.31 GHz, which covers WLAN, WIMAX, and WAIC applications. A parametric analysis is presented to identify the optimal value for all critical parameters. The proposed compact structure RDRA exhibits a stable omnidirectional pattern, good gain, adequate impedance bandwidth and good matching, making it suitable for the proposed next-generation wireless communication.

DATA AVAILABILITY STATEMENT

Available on Request. The datasets generated and/or analyzed during the current study are not publicly available due to the extent of the submitted research work. They are available from the corresponding author upon reasonable request.

REFERENCES

- [1] Bizan, M. S., Naseri, H., Pourmohammadi, P., Melouki, N., Iqbal, A., Denidni, T. A. (2023). Dual-band dielectric resonator antenna with filtering features for microwave and mm-wave applications. *Micromachines*, 14 (6), 1236. <https://doi.org/10.3390/mi14061236>
- [2] Illahi, U., Iqbal, J., Irfan, M., Ismail Sulaiman, M., Khan, M. A., Rauf, A., Bari, I., Abdullah, M., Muhammad, F., Nowakowski, G., Glowacz, A. (2022). A novel design and development of a strip-fed circularly polarized rectangular dielectric resonator antenna for 5G NR Sub-6 GHz band applications. *Sensors*, 22 (15), 5531. <https://doi.org/10.3390/s22155531>
- [3] Pan, Y., Zheng, S. (2015). A low-profile stacked dielectric resonator antenna with high-gain and wide bandwidth. *IEEE Antennas and Wireless Propagation Letters*, 15, 68-71. <https://doi.org/10.1109/LAWP.2015.2429686>
- [4] Patel, U., Upadhyaya, T. (2022). Four-port dual-band multiple-input multiple-output dielectric resonator antenna for Sub-6 GHz 5G communication applications. *Micromachines*, 13 (11), 2022. <https://doi.org/10.3390/mi13112022>
- [5] Jin, L., Tang, H., Shi, J., Lin, L., Xu, K. (2022). A dual-band, dual-polarized filtering antenna based on cross-shaped dielectric strip resonator. *Micromachines*, 13 (12), 2069. <https://doi.org/10.3390/mi13122069>
- [6] Qian, Y., Xie, S. (2022). Wideband circularly polarized filtering hybrid antenna. *Applied Sciences*, 12 (21), 11018. <https://doi.org/10.3390/app122111018>
- [7] Hu, P. F., Pan, Y. M., Zhang, X. Y., Hu, B. J. (2019). A compact quasi-isotropic dielectric resonator antenna with filtering response. *IEEE Transactions on Antennas and Propagation*, 67 (2) 1294-1299. <https://doi.org/10.1109/TAP.2018.2883611>
- [8] Pan, Y. M., Hu, P. F., Leung, K. W., Zhang, X. Y. (2018). Compact single-/dual-polarized filtering dielectric resonator antennas. *IEEE Transactions on Antennas and Propagation*, 66 (9), 4474-4484. <https://doi.org/10.1109/TAP.2018.2845457>
- [9] Li, Y., Zhao, Z., Tang, Z., Yin, Y. (2020). Differentially fed, dual-band dual-polarized filtering antenna with high selectivity for 5G sub-6 GHz base station applications. *IEEE Transactions on Antennas and Propagation*, 68 (4), 3231-3236. <https://doi.org/10.1109/TAP.2019.2957720>
- [10] Altaf, A., Jung, J.-W., Yang, Y., Lee, K.-Y., Yi, S.-H., Hwang, K. C. (2018). A 3-D meandered probe-fed dual-band circularly polarized dielectric resonator antenna. *Sensors*, 18 (8), 2421. <https://doi.org/10.3390/s18082421>
- [11] Awan, W. A., Hussain, N., Kim, S., Kim, N. (2022). A frequency-reconfigurable filter antenna for GSM, 4G-LTE, ISM, and 5G Sub-6 GHz band applications. *Sensors*, 22 (15), 5558. <https://doi.org/10.3390/s22155558>
- [12] Tang, H., Tong, C., Chen, J.-X. (2019). Multifunction applications of substrate integrated waveguide cavity in dielectric resonator antennas and reconfigurable circuits. *IEEE Transactions on Antennas and Propagation*, 67 (8), 5700-5704. <https://doi.org/10.1109/TAP.2019.2922439>
- [13] Boyuan, M., Pan, J., Wang, E., Yang, D. (2020). Wristwatch-style wearable dielectric resonator antennas for applications on limbs. *IEEE Access*, 8, 59837-59844. <https://doi.org/10.1109/ACCESS.2020.2983098>
- [14] Mazhar, W., Klymyshyn, D. M., Wells, G., Qureshi, A. A., Jacobs, M., Achenbach, S. (2019). Low-profile artificial grid dielectric resonator antenna arrays for mm-wave applications. *IEEE Transactions on Antennas and Propagation*, 67 (7), 4406-4417. <https://doi.org/10.1109/TAP.2019.2907610>
- [15] Iqbal, J., Illahi, U., Yasin, M. N., Albreem, M. A., Akbar, F. M. (2022). Bandwidth enhancement by using parasitic patch on dielectric resonator antenna for sub-6 GHz 5G NR bands application. *Alexandria Engineering Journal*, 61 (6), 5021-5032. <https://doi.org/10.1016/j.aej.2021.09.049>
- [16] Mishra, N. K., Das, S., Vishwakarma, D. K. (2019). Beam steered linear array of cylindrical dielectric resonator antenna. *AEU - International Journal of Electronics and Communications*, 98, 106-113. <https://doi.org/10.1016/j.aeue.2018.11.011>
- [17] Anuar, S. U., Jamaluddin, M. H., Din, J., Kamardin, K., Dahri, M. H., Idris, I. H. (2020). Triple band MIMO dielectric resonator antenna for LTE applications. *AEU - International Journal of Electronics and Communications*, 118, 153172. <https://doi.org/10.1016/j.aeue.2020.153172>
- [18] Baldazzi, E., Al-Rawi, A., Cicchetti, R., Smolders, A. B., Testa, O., van Coevorden Moreno, C. D., Caratelli, D. (2020). A high-gain dielectric resonator antenna with plastic-based conical horn for millimeter-wave applications. *IEEE Antennas and Wireless Propagation Letters*, 19 (6), 949-953. <https://doi.org/10.1109/LAWP.2020.2984565>

- [19] Ahmad, Z., Hesselbarth, J. (2018). On-chip dual-polarized dielectric resonator antenna for millimeter-wave applications. *IEEE Antennas and Wireless Propagation Letters*, 17 (10), 1769-1772.
<https://doi.org/10.1109/LAWP.2018.2865453>
- [20] Chen, H. N., Song, J.-M., Park, J.-D. (2019). A compact circularly polarized MIMO dielectric resonator antenna over electromagnetic band-gap surface for 5G applications. *IEEE Access*, 7, 140889-140898.
<https://doi.org/10.1109/ACCESS.2019.2943880>
- [21] Mukherjee, B., Patel, P., Mukherjee, J. (2020). A review of the recent advances in dielectric resonator antennas. *Journal of Electromagnetic Waves and Applications*, 34 (9), 1095-1158.
<https://doi.org/10.1080/09205071.2020.1744484>
- [22] Mohammed, A. S. B., Kamal, S., Ain, M. F., Ahmad, Z. A., Ullah, U., Othman, M., Hussin, R., Ab Rahman, M. F. (2019). Micro strip patch antenna: A review and the current state of the art. *Journal of Advanced Research in Dynamical and Control Systems*, 11 (07-Special Issue), 510-524.
- [23] Kiani, S. H., Iqbal, A., Wong, S. W., Savci, H. S., Alibakhshikenari, M., Dalarsson, M. (2022). Multiple elements MIMO antenna system with broadband operation for 5th generation smart phones. *IEEE Access*, 10, 38446-38457.
<https://doi.org/10.1109/ACCESS.2022.3165049>
- [24] Bari, I., Iqbal, J., Ali, H., Rauf, A., Bilal, M., Jan, N., Illahi, U., Arif, M., Khan, M. A., Ghoniem, R. M. (2022). Bandwidth enhancement and generation of CP of Yagi-Uda-shape feed on a rectangular DRA for 5G applications. *Micromachines*, 13 (11), 1913.
<https://doi.org/10.3390/mi13111913>
- [25] Illahi, U., Iqbal, J., Sulaiman, M. I., Alam, M. M., Su'ud, M. M., Jamaluddin, M. H. (2019). Singly-fed rectangular dielectric resonator antenna with a wide circular polarization bandwidth and beamwidth for WiMAX/satellite applications. *IEEE Access*, 7, 66206-66214.
<https://doi.org/10.1109/ACCESS.2019.2917702>

Received September 16, 2023
Accepted November 02, 2023